

On low-sampling-rate Kramers-Moyal coefficients

C. Anteneodo

*Department of Physics, PUC-Rio and
National Institute of Science and Technology for Complex Systems
Rua Marquês de São Vicente 225, Gávea,
CEP 22453-900 RJ, Rio de Janeiro, Brazil*

S.M. Duarte Queirós

*Centro de Física do Porto
Rua do Campo Alegre, 687, 4169-007 Porto, Portugal
(Dated: February 15, 2022)*

We analyze the impact of the sampling interval on the estimation of Kramers-Moyal coefficients. We obtain the finite-time expressions of these coefficients for several standard processes. We also analyze extreme situations such as the independence and no-fluctuation limits that constitute useful references. Our results aim at aiding the proper extraction of information in data-driven analysis.

PACS numbers: 05.10.Gg, 05.40.-a, 02.50.Ey, 89.65.Gh

Keywords: finite-time, Kramers-Moyal expansion, Itô-Langevin equation

I. INTRODUCTION

The study of systems composed of a large number of degrees of freedom was endowed a definitive means of reasoning with the introduction of the differential stochastic dynamical framework about a century ago [1]. Specifically, differential stochastic dynamics allows one to describe the time evolution of a given observable as a function of macroscopic variables of the system as well as non-deterministic ones. The latter are expressed in terms of noise(s), reflecting the microscopic features of the system, whose univocal description is beyond the bounds of possibility [2, 3]. Despite the impossibility of a deterministic description of the evolution of the observable, one can successfully obtain time dependent statistical details. Undeniably, Einstein's and Bachelier's groundbreaking works, respectively on Brownian motion [4] and stock price movements [5], are outstanding examples of the relevance of differential stochastic dynamics in diverse fields.

The inference of a differential stochastic process is generically made from statistical features such as statistical moments, correlation functions and probability density functions built from a time series of measurements. In particular, a well established theoretical background for identifying the stochastic dynamics exists for the important class of processes following the Markov property [2, 3]. However, in practice, several hindrances arise. Specifically, besides matters related to the finite size of data sets [6] and to the direct error of the measurements (associated with the quality of the equipments and/or their calibration [7]), the sample rating (the spell between logged measurements) plays a crucial role in the determination of actual underlying stochastic process. As a matter of fact, we are generally left a set of snapshots reproducing a fraction of the events that occurred in the continuous time process from which the dynamics is due to be determined. In any case, it would be important to

compare the acquisition interval with the characteristic times of the process to determine whether the Kramers-Moyal (KM) coefficients estimates are trustworthy. In this respect, another difficulty is that the characteristic times are not always known beforehand, although they can be estimated, e.g., through the computation of auto-correlation functions. Moreover, when the sampling interval is found to be too long compared with the characteristic timescales, for suitably uncovering the process, it is not always possible to upgrade it, particularly for historical data. For such cases, it is therefore of primary importance a careful analysis of the impact of the time interval τ of data sampling on the observable finite-time KM coefficients, specially as one approaches the independence limit.

For a Markovian timeseries, one can obtain the evolution equation for the conditioned probability density (PDF) by computing the KM coefficients,

$$D_k(x_0) = \lim_{\tau \rightarrow 0} \tilde{D}_k(x_0, \tau), \quad (1)$$

with

$$\begin{aligned} \tilde{D}_k(x_0, \tau) &= \frac{1}{k! \tau} \int dx P(x, \tau | x_0, 0) [x(\tau) - x_0]^k \\ &\equiv \frac{1}{k! \tau} \langle [x(\tau) - x_0]^k \rangle, \\ &= \frac{1}{k! \tau} \sum_{j=0}^k \binom{k}{j} \langle x^j \rangle (-x_0)^{k-j}, \end{aligned} \quad (2)$$

where we have already assumed that the coefficients are (at least locally) stationary (for non-stationary data-sets see Ref. [6]). Aiming to simplify the notation, we denote the statistical averages conditioned to the initial value x_0 : $\langle \cdots \rangle|_{x=x_0} \equiv \langle \cdots \rangle$, while we will reserve $\langle \cdots \rangle_u$ for usual stationary unconditioned averages.

In practice, only the finite-time estimates $\tilde{D}_k(x_0, \tau)$ can be directly computed, with τ limited by the minimal

time interval, τ_{min} , of data acquisition. Furthermore, when the sampling interval τ is larger than the correlation time, i.e., the PDF $P(x, \tau|x_0, 0)$ becomes unconditioned and under stationarity, one gets,

$$\begin{aligned}\tilde{D}_k^{indep}(x_0, \tau) &= \frac{1}{k!\tau} \int dx P(x) [x - x_0]^k \\ &\equiv \frac{1}{k!\tau} \langle [x(\tau) - x_0]^k \rangle_u, \\ &= \frac{1}{k!\tau} \sum_{j=0}^k \binom{k}{j} \langle x^j \rangle_u (-x_0)^{k-j}. \quad (3)\end{aligned}$$

Notice that, in Eq. (3) the stationary averages are unconditioned, hence do not depend on x_0 , differently from Eq. (2). Therefore, Eq. (3) represents a k -order polynomial in x_0 , no matter how complex the intrinsic coefficients D_k are. In practical applications, this feature introduces a complete uncertainty on the actual form of the intrinsic coefficients, in the absence of a model *a priori* [8].

In this manuscript we obtain the finite-time estimates for several standard processes described by Itô-Langevin stochastic differential equations,

$$dx = D_1(x)dt + \sqrt{2D_2(x)}dW_t, \quad (4)$$

where W_t is a standard Wiener process. In previous work [9], this task was accomplished for the particular class of processes with $D_1 = -ax$ and $D_2 = Ax^2 + C$, by means of Itô-Taylor expansions. Herein, we will consider a larger class of processes following two different approaches. The first one, based on the solution of the evolution equation of the raw statistical moments, represents a simplification regarding the whole process of appraising the finite-time coefficients when the drift is linear. Second, we employ the Fokker-Planck adjoint operator technique that is useful for processes with nonlinear drifts, for instance.

Furthermore, we will analyze the extreme instances of no-fluctuations and independence. The deterministic limit (absence of fluctuations) is relevant in stochastic dynamical systems since it provides a reference on the functional behavior of quantities that can be perturbed by augmenting the intensity (broadness) of the noise. In the meanwhile, the independence limit sets the bounds expected for large acquisition interval and/or large noise intensity.

Although it is not always possible a direct inversion of the finite-time estimates to extract the intrinsic ones, the expressions herein obtained can be contrasted against the observed KM coefficients, allowing the identification of the underlying process as well as the associated parameter values.

II. ESTIMATING CONDITIONAL MOMENTS

Given the Fokker-Planck equation (FPE) for $P \equiv P(x, t|x_0, 0)$

$$\partial_t P = -\partial_x [D_1 P] + \partial_{xx} [D_2 P], \quad (5)$$

the evolution equation for a mean value can be obtained by multiplying both sides of Eq. (5) times the quantity to be averaged and integrating by parts with suitable boundary conditions (vanishing at the boundaries). In this way, the equations for the moments have the form

$$\frac{d\langle x^n \rangle}{dt} = n\langle x^{n-1} D_1(x) \rangle + n(n-1)\langle x^{n-2} D_2(x) \rangle. \quad (6)$$

If $D_1(x)$ is linear and $D_2(x)$ is at most quadratic, the equations for the moments can be successively solved from the lowest order $n = 1$ [10]. However, a hierarchy of equations depending on higher order moments generally arises. In such cases, one can still resort to approximate techniques such as hierarchy truncation, substitution of terms, etc. Alternatively, the conditional averages can be computed by means of the short-time solution expansion [2], which leads to

$$\langle Q(x) \rangle(x_0, \tau) = \sum_{n \geq 0} [L^\dagger(x)]^n Q(x)|_{x_0} \tau^n / n!, \quad (7)$$

where $L^\dagger(x) = D_1 \partial_x + D_2 \partial_{xx}$ is the (backwards) Fokker-Planck adjoint operator (see also [11]).

In the deterministic case, it is enough to solve Eq. (6) for the first moment, which becomes

$$\frac{d\langle x \rangle^{det}}{dt} = D_1(\langle x \rangle^{det}), \quad (8)$$

where the superindex stands for “deterministic” and whence we obtain the full range of values, $\langle x^k \rangle^{det} = (\langle x \rangle^{det})^k$. Then, the deterministic part of \tilde{D}_k , with $k \geq 1$, is

$$\tilde{D}_k^{det} = \frac{1}{k!\tau} (\langle x \rangle^{det} - x_0)^k = \frac{\tau^{k-1}}{k!} (\tilde{D}_1^{det})^k. \quad (9)$$

Let us note that the deterministic \tilde{D}_k are non-null functions, although they vanish in the limit $\tau \rightarrow 0$ except for $k = 1$. Nevertheless, we should bear in mind that for not too small τ the deterministic part can dominate over the noise contribution. This represents another drawback one may face in a practical application. In fact, if the noise is small, the deterministic contribution to \tilde{D}_k may screen the information on the noise.

III. LINEAR DRIFT

Let us first consider the case of linear drift,

$$D_1(x) = -ax + b, \quad (10)$$

with $a > 0$ assuring the existence of a stationary solution. As a matter of fact, a raft of phenomena are described by an exponential relaxation, which is concomitant with a parabolic drift potential [3]. From Eq. (6) one has

$$\frac{d\langle x \rangle}{dt} = -a\langle x \rangle + b, \quad (11)$$

whose solution is

$$\langle x(\tau) \rangle = x_0 z + \frac{b}{a}(1 - z), \quad (12)$$

assuming the initial condition $\langle x(0) \rangle = x_0$ and defining $z \equiv e^{-a\tau}$. Hence, according to Eq. (2),

$$\tilde{D}_1(x_0, \tau) = -\left(x_0 - \frac{b}{a}\right) \frac{1 - z}{\tau}, \quad (13)$$

that in the limit $\tau \rightarrow 0$ recovers D_1 . The opposite limit of independence yields $-(x_0 - b/a)/\tau$ in accordance with Eq. (3).

It is noteworthy that Eq. (13) is independent of the particular form of D_2 . This is due to the fact that in (and only in) the linear case, Eq. (11) coincides with its deterministic version, Eq. (8), hence $\tilde{D}_1 = \tilde{D}_1^{det}$. For other forms of the deterministic part of the stochastic differential equation, the derivative of $\langle x \rangle$ with respect to the time is equal to more complex expressions which depend on higher-order moments and/or powers of the first conditional moment. Despite the slope evolution with τ , it is worth noting that the finite- τ drift preserves the linear form of the intrinsic D_1 .

Equation (12) also allows one to estimate the conditional two-time covariance function given by [3],

$$\begin{aligned} K(\tau, x_0) &= \int dx x x_0 P(x, t | x_0, 0) = x_0 \langle x(\tau) \rangle \\ &= x_0^2 z + x_0 \frac{b}{a}(1 - z), \end{aligned} \quad (14)$$

that exponentially decays towards the long-time average. Still one has to average over initial conditions x_0 to find,

$$K(\tau) = \int dx dx_0 x x_0 P(x, t; x_0, 0) = \int dx_0 K(\tau, x_0) P(x_0),$$

where $P(x_0)$ is usually the steady PDF. However, any choice of $P(x_0)$ will not alter the exponential character of the correlations since the integration is not carried out over time. In addition, the correlations are only ruled by the drift and do not depend on the noise amplitude. It is straightforward to understand that this quirk comes to pass because of the functional properties of the conditional average.

1. Second and higher order conditional moments for quadratic noise intensity

If together with drift linearity the noise intensity is second-order polynomial,

$$D_2(x) = Ax^2 + Bx + C, \quad (15)$$

with parameters such that $D_2(x) > 0$, then each evolution Eq. (6) is linearly coupled to those of lower order only. In this case the equations can be solved one after another. In particular, for the second moment, one has,

$$\frac{d\langle x^2 \rangle}{dt} = 2(-(a - A)\langle x^2 \rangle + (b + B)\langle x \rangle + C). \quad (16)$$

Thus, we just need to solve a non-homogeneous 1st order differential equation of the form

$$f' = \hat{A}f + \hat{B}e^{-\alpha t} + \hat{C}, \quad (17)$$

whose solution, given the initial condition $f(0)$, is

$$\begin{aligned} f(t) &= \frac{\alpha \hat{C} + \hat{A}(\hat{B} + \hat{C} + (\alpha + \hat{A})f(0))}{\hat{A}(\alpha + \hat{A})} e^{\hat{A}t} \\ &\quad - \frac{\hat{B}}{\alpha + \hat{A}} e^{-\alpha t} - \frac{\hat{C}}{\hat{A}}. \end{aligned} \quad (18)$$

Therefore, $\langle x^2(\tau) \rangle = f(\tau)$ with the identifications,

$$\hat{A} = -2(a - A),$$

$$\hat{B} = 2(b + B)(x_0 - b/a),$$

$$\hat{C} = 2(b + B)b/a + 2C,$$

and $\alpha = a$, following Eqs. (16) and (12), and the initial condition $f(0) = x_0^2$. Namely,

$$\begin{aligned} \langle x^2(\tau) \rangle &= z^2 w x_0^2 + 2 \frac{b + B}{a - 2A} (z - z^2 w) x_0 \\ &\quad + \frac{b(b + B)}{a(a - A)(a - 2A)} (az^2 w - 2(a - A)z + a - 2A) \\ &\quad + \frac{C}{a - A} (1 - z^2 w), \end{aligned} \quad (19)$$

where $z \equiv e^{-a\tau}$ and $w \equiv e^{2A\tau}$.

The finite- τ second KM coefficient can be obtained by means of Eq. (2) with $\langle x(\tau) \rangle$ and $\langle x^2(\tau) \rangle$ given by Eqs. (12) and (19), respectively. Explicitly, we find

$$\begin{aligned} \tilde{D}_2(x_0, \tau) &= \frac{1}{2\tau} \left([1 - 2z + z^2 w] x_0^2 \right. \\ &\quad + 2 \left[\frac{b + B}{a - 2A} (z - z^2 w) + \frac{b}{a} (z - 1) \right] x_0 \\ &\quad + \frac{b(b + B)(az^2 w - 2(a - A)z + a - 2A)}{a(a - A)(a - 2A)} \\ &\quad \left. + \frac{C}{a - A} (1 - z^2 w) \right). \end{aligned} \quad (20)$$

When $\tau \rightarrow 0$, $\tilde{D}_2 \rightarrow D_2$, while for $a\tau \gg 1$, Eq. (3) is verified.

These results permit one to embrace many fundamental models such as Ornstein-Uhlenbeck, Feller and

harmonic drift with additive-(linear)multiplicative noise. Also in finance, in most well-known models of volatility ($\sigma = \sqrt{x}$), the drift is linear and $D_2 = D|x|^\beta$, with $\beta = 0$ (Ornstein-Uhlenbeck process), 1 (square-root, Feller or Cox-Ingersoll-Ross model) and 2 (Hull and White model).

Let us also recall that for the linear drift, its finite-time expressions are also linear in x_0 . Similarly, with linear drift and $\beta = 0, 1, 2$ the dependence of \tilde{D}_2 on x_0 is quadratic. As a matter of fact, a similar scenario holds for k th-order finite-time KM coefficients. In other words, the k th-order KM coefficients are polynomials of order k , whose coefficients depend on τ . Thus, it is not simple to nimbly rescue the value of β just by identifying the polynomial order of the observed coefficients.

For the quadratic noise intensity, the evolution equations of higher order conditional moments, from Eq. (6), are

$$\frac{d\langle x^n \rangle}{dt} = A_n \langle x^n \rangle + B_n \langle x^{n-1} \rangle + C_n \langle x^{n-2} \rangle, \quad (21)$$

where

$$\begin{aligned} A_n &= n[(n-1)A - a]; \\ B_n &= n[(n-1)B + b]; \\ C_n &= n(n-1)C. \end{aligned}$$

High-order KM coefficients are particularly relevant as well. In other words, for the present class of Markovian processes the Pawula theorem [2] implies that they must vanish. In the absence of any other reason to discard the validity of Chapman-Kolmogorov approach, if the finite-time conditional higher-moments are non-null, it is important to probe whether it is the outcome of a finite-time effect. Let us restrain our calculations to the explicit formulae of the third and fourth coefficients in two important cases: (i) the reversion to a null value in the absence of coupling between additive and (linear) multiplicative white noises ($b = 0$ and $B = 0$) and (ii) the Feller process.

(i) For the additive-multiplicative process with $b = 0$ and $B = 0$, notice that Eq. (6) with $n = 3$ has the same form of Eq. (17), through the identification $\hat{A} = -3(a - 2A)$, $\hat{B} = 6Cx_0$, $\hat{C} = 0$ and $\alpha = a$, and the initial condition $f(0) = x_0^3$, yielding

$$\langle x^3(\tau) \rangle = \frac{3x_0C}{a-3A}(z - (zw)^3) + x_0^3(zw)^3. \quad (22)$$

Then, according to Eq. (2), one has

$$\tilde{D}_3(x_0, \tau) = \frac{1}{6\tau} \left(\langle x^3(\tau) \rangle - 3x_0 \langle x^2(\tau) \rangle + 3x_0^2 \langle x(\tau) \rangle - x_0^3 \right), \quad (23)$$

where the averaged quantities are given by Eqs. (22), (19) and (12), respectively.

For the fourth moment, Eq. (6) with $n = 4$ has the same form of Eq. (17), through the identification $\hat{A} =$

$4(3A - a)$, $\hat{B} = 12C^2/(A - a) + 12Cx_0^2$, $\hat{C} = -12C^2/(A - a)$ and $\alpha = 2(a - A)$, together with the initial condition $f(0) = x_0^4$, yielding

$$\begin{aligned} \langle x^4(\tau) \rangle &= z^4 w^6 x_0^4 + \frac{6C(z^2 w - z^4 w^6)}{a - 5A} x_0^2 \\ &+ 3C^2 \frac{(a - A)z^4 w^6 - 2(a - 3A)z^2 w + a - 5A}{(a - A)(a - 3A)(a - 5A)}. \end{aligned} \quad (24)$$

Thus,

$$\begin{aligned} \tilde{D}_4(x_0, \tau) &= \frac{1}{24\tau} \left(\langle x^4(\tau) \rangle - 4x_0 \langle x^3(\tau) \rangle \right. \\ &\left. + 6x_0^2 \langle x^2(\tau) \rangle - 4x_0^3 \langle x(\tau) \rangle + x_0^4 \right), \end{aligned} \quad (25)$$

is obtained by substitution of the averaged quantities Eqs. (24), (22), (19) and (12). The present results generalize those previously obtained for the particular case $D_1 = -ax$ (with $a > 0$) and $D_2 = Ax^2 + C$ in [9].

(ii) For the Feller process ($A = C = 0$), by successive integration of Eqs. (21) and using (2) we find,

$$\begin{aligned} \tilde{D}_3(x_0, \tau) &= \frac{(1-z)^3}{6\tau} \left(-x_0^3 + 3 \frac{b - (b+2B)z}{a(1-z)} x_0^2 \right. \\ &\left. - 3 \frac{(b+B)(b - (b+2B)z)}{a^2(1-z)} x_0 + \frac{b(b+B)(b+2B)}{a^3} \right) \end{aligned} \quad (26)$$

and

$$\begin{aligned} \tilde{D}_4(x_0, \tau) &= \frac{(1-z)^4}{24\tau} \left(x_0^4 - 4 \frac{b - (b+3B)z}{a(1-z)} x_0^3 \right. \\ &+ 6 \frac{(b+2B)[(b+3B)z - 2(b+B)]z + b(b+B)}{a^2(1-z)^2} x_0^2 \\ &- 4 \frac{(b+B)(b+2B)(b - (b+3B)z)}{a^3(1-z)} x_0 \\ &\left. + \frac{b(b+B)(b+2B)(b+3B)}{a^4} \right). \end{aligned} \quad (27)$$

Considering that for the Feller process $\langle x \rangle_u^n = (B/A)^n \frac{\Gamma(b/B+n)}{\Gamma(b/B)}$, then the KM coefficients can be rewritten in terms of the unconditioned raw moments, which can be straightforwardly estimated from data, as follows,

$$\tilde{D}_1(x_0, \tau) = \frac{(1-z)}{\tau} \langle x - x_0 \rangle_u.$$

$$\tilde{D}_2(x_0, \tau) = \frac{(1-z)^2}{2\tau} \langle (x - x_0)^2 \rangle_u,$$

$$\begin{aligned} \tilde{D}_3(x_0, \tau) &= \frac{(1-z)^3}{6\tau} \langle (x - x_0)^3 \rangle_u \\ &+ \frac{z(1-z)^2}{\tau} \frac{\sigma_x^2}{\langle x \rangle_u^2} \langle x(x - x_0) \rangle_u x_0, \end{aligned}$$

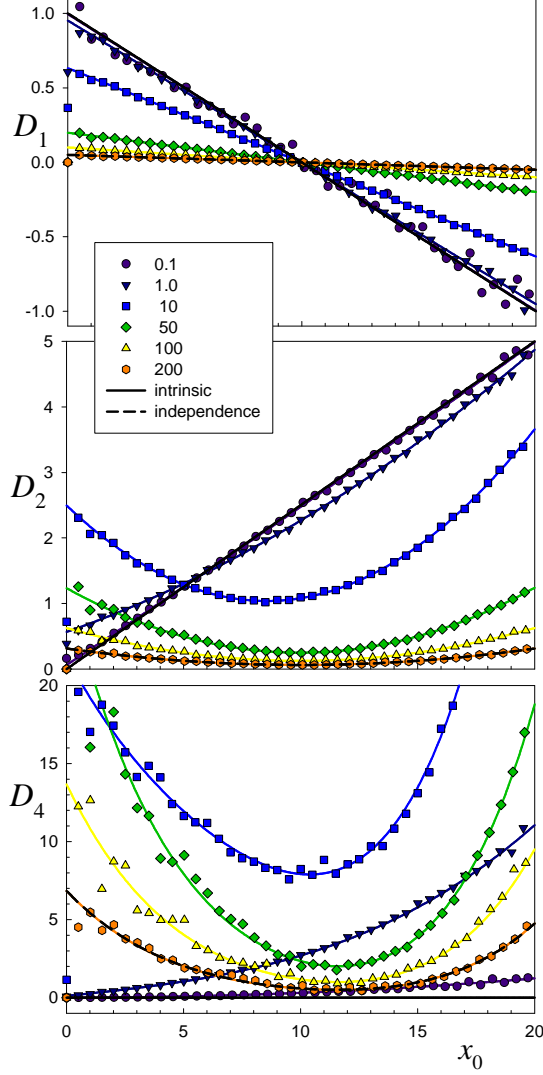


FIG. 1: Color online. Impact of τ on first, second and fourth finite-time KM coefficients for the process $dx = (-ax+b)dt + \sqrt{2Bx}dW$, with $a = 0.1$, $b = 1.0$ and $B = 0.25$. The values of τ used are indicated on the figure. Artificial timeseries were generated by means of the Euler algorithm with $dt = 10^{-3}$ and 10^6 data points of the timeseries were considered for the computation of KM coefficients in each case. Symbols correspond to numerical estimates and the associated colored solid lines to the theoretical expressions for finite-time coefficients given by Eqs. (13), (20) and (27). Black solid lines correspond to the intrinsic coefficients $D_1 = -ax + b$, $D_2 = Bx$ and $D_4 = 0$ and black dashed lines (practically coinciding with the curves for $\tau = 200$), to the independence limit forms given by Eq. (3) with $\tau = 200$

and

$$\begin{aligned} \tilde{D}_4(x_0, \tau) &= \frac{(1-z)^4}{24\tau} \left\langle (x-x_0)^4 \right\rangle_u \\ &+ \frac{z(1-z)^3}{2\tau} \frac{\sigma_x^2}{\langle x \rangle_u^2} \left\langle x(x-x_0)^2 \right\rangle_u x_0 + \frac{z^2(1-z)^2}{2\tau} \frac{\sigma_x^2}{\langle x \rangle_u^2} x_0^2 \end{aligned}$$

FIG. 2: Color online. Impact of the noise intensity on the first and second finite-time KM coefficients for the same process of Fig. 1. In all cases $\tau = 5$ and the different values of B are indicated on the figure. Black solid lines correspond to the intrinsic coefficients, black dashed lines to the independence limit forms at $\tau = 5$ and black dotted lines to the deterministic forms (Eq. (9)) at $\tau = 5$. Symbols correspond to numerical estimates and the associated colored (thin) solid lines to the theoretical expressions for finite-time coefficients given by Eqs. (13) and (20). In the lower panel the inset shows the same data in log-linear scales.

where $\sigma_x^2 = \langle x^2 \rangle_u - \langle x \rangle_u^2$.

In Fig. 1, we exemplify the behavior of \tilde{D}_1 , \tilde{D}_2 and \tilde{D}_4 for the Feller process $dx = (-ax+b)dt + \sqrt{2Bx}dW$ (that is $A = C = 0$, or also $\beta = 1$) as the independence limit is approached. Notice the variety of behaviors that can be observed even for not too large τ . The slope of the linear \tilde{D}_1 changes with τ taking the values $-(1-z)/\tau$, while \tilde{D}_2 soon becomes quadratic with τ . Also \tilde{D}_4 largely departs from the intrinsic null value. For all the coefficients, the independence limit is practically attained at $\tau \simeq 200$ ($\tau \gg 1/a = 10$).

Figure 2 illustrates the impact of the intensity of noise on the finite-time estimates. Noise intensity does not affect \tilde{D}_1 which coincides with the deterministic straight line. \tilde{D}_2 largely disagrees with the true form D_2 , departing towards the independence limit, for large noise intensity, and towards the deterministic limit for small noise. Of course, as one approaches the deterministic (no-fluctuations) limit the range of x_0 shrinks around the deterministic (equilibrium) value.

When the drift is linear, whatever the noise intensity, the parameters a and b can be unraveled by a linear fit to the observed \tilde{D}_1 : the value of the slope $-(1-z)/\tau$ allows one to determine the parameter a , once τ is known, while the abscissa at which \tilde{D}_1 vanishes corresponds to b/a . That is, if the observed drift can be considered linear in good approximation, a direct inversion of \tilde{D}_1 to obtain the intrinsic D_1 is possible. This will also facilitate the obtention of the functional form (and parameter values) of D_2 .

2. Non-quadratic noise intensity

For $\beta \neq 0, 1, 2$, or more generally for non-quadratic D_2 , the finite-time \tilde{D}_2 are also non quadratic in x . The equation for the second moment, following Eq. (6),

$$\frac{d\langle x^2 \rangle}{dt} = -2a\langle x^2 \rangle + 2b\langle x \rangle + 2\langle D_2(x) \rangle \quad (28)$$

cannot be solved straightforwardly in this case.

Let us consider the especial case with $\beta = 3$ (known as 3/2-model) used as a volatility model as well [12]. For small noise intensity, one can find the correction c_2 to the deterministic part of $\langle x^2 \rangle$ by means of expansion (7), taking $Q(x) = x^2$. By identifying the general form of the coefficients of τ^n , with the aid of algebraic manipulation programs, we obtain

$$c_2 = \frac{C}{a^4} (b^3 + 6b^2(ax_0 - b)z + (3b^3 - 6a^2bx_0^2 + 2a^3x_0^3)z^2 + 6ab\tau(ax_0 - b)^2z^2 - 2z^3(ax_0 - b)^3). \quad (29)$$

Then

$$\langle x^2 \rangle = (\langle x \rangle^{det})^2 + c_2 + \mathcal{O}(C^2) \quad (30)$$

and on that account,

$$\tilde{D}_2 = \frac{\tau}{2}(\tilde{D}_1^{det})^2 + \frac{c_2}{2\tau} + \mathcal{O}(C^2), \quad (31)$$

which in the limit $\tau \rightarrow 0$ tends to $D_2 \equiv Cx^3$ as expected.

IV. NONLINEAR DRIFT

As in the case of linear drift and non-quadratic noise, if the drift is nonlinear, the equations for the moments cannot be solved successively from the lowest order. Moreover, the useful independence of the evolution equation for $\langle x(t) \rangle$ on higher order statistical moments, which are noise dependent, fails. Consequently, the existence of a nonlinear drift introduces a troublesome relation between \tilde{D}_1 and the noise as well as a dependence of the correlation function on the same noise. However, we can still use the calculations at the deterministic limit to represent the upper bound which is quite reliable for the cases

presenting small noise intensity. Explicitly, if the contribution of diffusion is neglected, the evolution is almost deterministic. Accordingly, we will solve the deterministic equation for the first moment whereas for higher order moments we will take into account the lowest order correction due to noise.

Let us consider a process with cubic drift [13] also called Bernoulli oscillator,

$$dx = (-ax - bx^3)dt + \sqrt{2C}dW_t, \quad (32)$$

where $b, C \geq 0$. When $a < 0$ the system represents a stochastic motion in a bistable potential. The statistical moments of this stochastic system were early studied within a variational approach context [14]. However, this method lands up introducing an extra (fitting) parameter which we adamantly want to avoid, since it would increase the level of uncertainty of the results.

Figure 3 exhibits the first, second and fourth finite-time KM moments, obtained for different values of the sampling interval τ . Notice that, with increasing τ , \tilde{D}_1 tends to a linear form that can erroneously lead to assume that the drift is linear. However, under this assumption, the inversion of \tilde{D}_1 should give incongruous results for D_1 , thus leading to discard the linearity of D_1 . For small noise intensity, the deterministic expression fitted (with two fitting parameters a and b) to the observed \tilde{D}_1 allows to recover D_1 . Notice also the complex influence of D_1 on the higher order coefficients, leading to forms with two minima, in contrast with the linear drift case.

By integration of Eq. (8), one obtains the deterministic expression,

$$\tilde{D}_1^{det}(x_0, \tau) = \left(\frac{e^{-a\tau}}{\sqrt{1 + bx_0^2(1 - e^{-2a\tau})}/a} - 1 \right) \frac{x_0}{\tau}, \quad (33)$$

that does not preserve the original simple cubic form underscoring the unique character of the linear drift. In the limit $b \rightarrow 0$, one recovers the linear case studied above. The case where b is a perturbative parameter may be of interest for systems in the vicinity of a phase transition, such as in Refs. [15]. In the limit $a \rightarrow 0$, Eq. (33) becomes,

$$\tilde{D}_1^{det}(x_0, \tau) = \left(\frac{1}{\sqrt{1 + 2bx_0^2\tau}} - 1 \right) \frac{x_0}{\tau}. \quad (34)$$

Independent of the signal of a , for short τ , $\tilde{D}_1^{det}(x_0, \tau)$ is equal to $-ax - bx^3$. For large values of τ , the picture depends on whether a is positive or negative. In the former case, which corresponds to a single well potential, \tilde{D}_1^{det} is defined by a straight line,

$$\tilde{D}_1^{det}(x_0, \tau) = -\frac{x_0}{\tau}, \quad (35)$$

which corresponds to the independence limit. Meanwhile, in the latter case, which entails bi-stable poten-

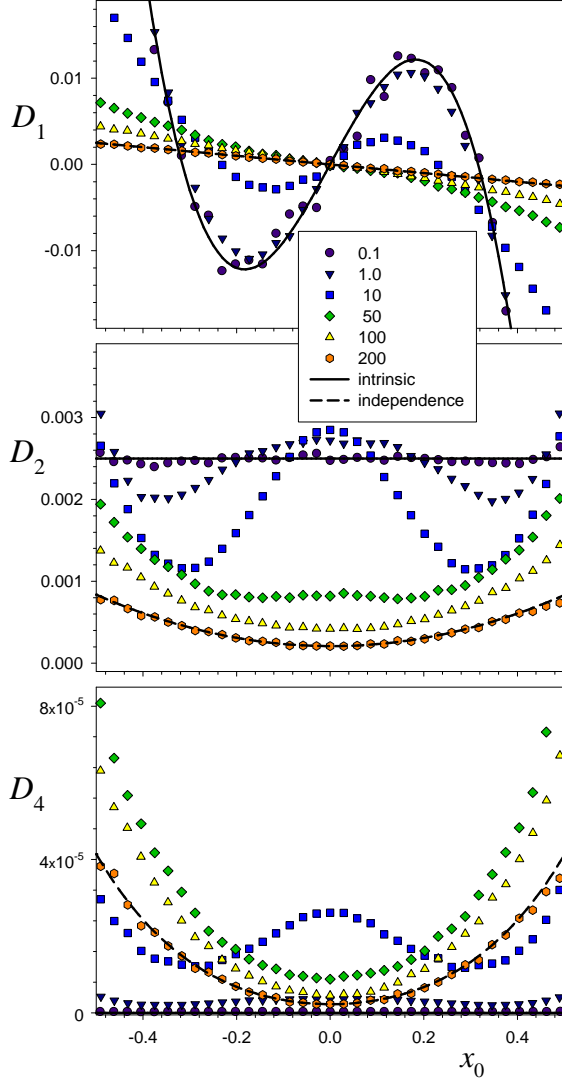


FIG. 3: Color online. Impact of τ on the first, second and fourth finite-time KM coefficients, for the process defined by Eq. (32), with $a = -0.1$, $b = 1$ and $C = 0.0025$. The values of τ are indicated on the figure. Symbols correspond to numerical estimates. Black solid lines correspond to the intrinsic coefficients $D_1 = -ax - bx^3$, $D_2 = C$ and $D_4 = 0$, while black dashed lines to the independence limit forms at $\tau = 200$.

tials, one obtains,

$$\tilde{D}_1^{det}(x_0, \tau) = \left(\frac{e^{|a|\tau}}{\sqrt{1 + b x_0^2 (e^{2|a|\tau} - 1)/|a|}} - 1 \right) \frac{x_0}{\tau}. \quad (36)$$

In this case, for large values of $|a|\tau$, one can describe the limits corresponding to large values of $b/|a| x_0^2 e^{2|a|\tau}$,

$$\tilde{D}_1^{det}(x_0, \tau) \approx \sqrt{\frac{|a|}{b}} \frac{1}{\tau} - \frac{x_0}{\tau}, \quad (37)$$

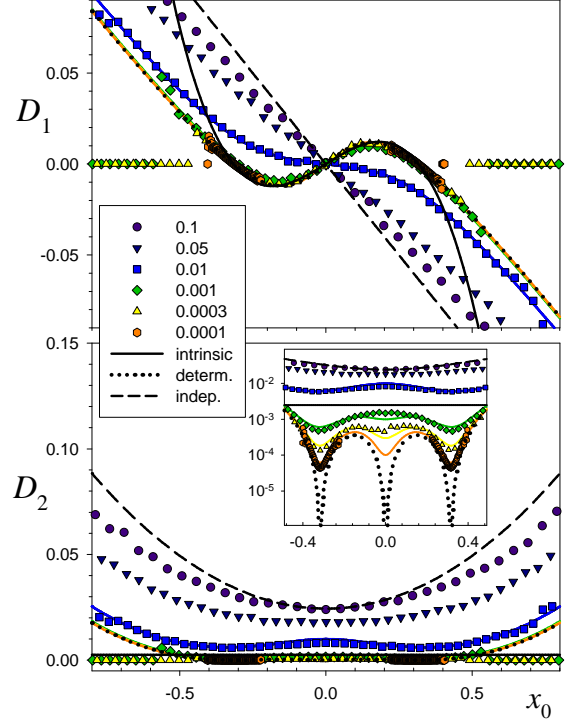


FIG. 4: Color online. Impact of the noise intensity on the first and second finite-time KM coefficients, for the same process of Fig. (3). In all cases $\tau = 5$, and the different values C used are indicated on the figure. Black solid lines correspond to the intrinsic coefficients, black dashed lines to the independence limit at $\tau = 5$, and black dotted lines to the deterministic forms (9) at $\tau = 5$. Symbols correspond to numerical estimates and the associated colored lines to the approximations for small noise intensity given by Eqs. (42) and (45), respectively. In the lower panel the inset shows the same data in log-linear scales. For the smallest noise intensity two different initial conditions were used to fill both potential wells.

and for small values of the same quantity,

$$\tilde{D}_1^{det}(x_0, \tau) \approx \frac{\exp[|a|\tau] - 1}{\tau} x_0 - \frac{b \exp[3|a|\tau]}{2|a|\tau} x_0^3. \quad (38)$$

As a result, we can verify that the polynomial dependence of $\tilde{D}_1^{det}(x_0, \tau)$ is preserved for the central region that dwindles as the sampling rate increases resulting in the straight line limit (37), which describes the full dependence (beyond relaxation scale) situation.

In the generic case $D_1 = -h x^n$ (with $h, n > 0$), the solution to Eq. (8) is,

$$\tilde{D}_1^{det}(x_0, \tau) = \left(\frac{1}{(1 + (n-1)h x_0^{n-1} \tau)^{\frac{1}{n-1}}} - 1 \right) \frac{x_0}{\tau}, \quad (39)$$

which includes Eq. (34) as a particular case (for $n = 3$) and also the linear case with $b = 0$ (for $n = 1$). In the latter instance it is provable that the exponential

functional dependence is recovered. For all the cases and in the limit $\tau \rightarrow 0$, one recovers $D_1(x)$ whereas in the opposite limit $\tau \rightarrow \infty$, one gets $-x/\tau$.

For small fluctuations, higher order finite- τ KM moments are dominated by the deterministic part given by Eq. (9) with further corrections dependent on the noise.

For the cubic drift, in the presence of small fluctuations, such that $C \sim a$,

$$\langle x \rangle = \langle x \rangle^{det} + c_1 + \mathcal{O}(C^2, aC, a^2), \quad (40)$$

with,

$$c_1 = -Cb x_0 \tau^2 \frac{3 + 4y + 2y^2}{(1 + 2y)^{5/2}} \quad (41)$$

and $y = bx_0^2 \tau$. Then,

$$\tilde{D}_1 = \tilde{D}_1^{det} + \frac{c_1}{\tau} + \mathcal{O}(C^2, aC, a^2), \quad (42)$$

where \tilde{D}_1^{det} is given by Eq. (33).

Similarly, for the second moment we found the first correction to the deterministic part

$$\langle x^2 \rangle = (\langle x \rangle^{det})^2 + c_2 + \mathcal{O}(C^2, aC, a^2), \quad (43)$$

with

$$c_2 = \frac{2C\tau}{(1 + 2y)^3}. \quad (44)$$

Then, finally

$$\tilde{D}_2 = \frac{\tau}{2}(\tilde{D}_1^{det})^2 + \frac{c_2 - 2x_0 c_1}{2\tau} + \mathcal{O}(C^2, aC, a^2), \quad (45)$$

which verifies that \tilde{D}_2 tends to $D_2 \equiv C$ as $\tau \rightarrow 0$.

Figure 4 shows the impact of the intensity of noise on the finite-time estimates. In contrast to the linear drift case, here the noise influences \tilde{D}_1 , in such a way that as the intensity of noise C increases, \tilde{D}_1 approaches the independence limit even for small sampling rates. This could be attributed to the decorrelating role of noise (it is worth regarding that \tilde{D}_1 already depends on the noise for non-linear potentials). Similarly to the linear case, \tilde{D}_2 largely disagrees with the true form D_2 , departing towards the independence limit, for large noise intensity, and towards the deterministic limit for small noise. Notice that if the intensity of noise is too small, one of the wells of the potential may become inaccessible. Precisely, let us focus on the insets in the lower panel of fig. 4. When one is in the no-fluctuation regime the system is characterized by three fixed points, namely one unstable (at $x = 0$, which prevails if and only if $x = 0$ is the initial condition) and two stable points (at $x = \pm\sqrt{a/b}$). Minimal noise is able to make the observable, which we can envisage as a virtual particle, move off the unstable point to one of the wells, each one defined by one of the remaining extremes (minima), but it gives a very little rate of transition between the regions of stability.

As the noise intensity augments, the rate of transition increases as well and we are able to detect the finite values of the KM moments in the vicinity of the unstable point. This can be adduced by computing the first non-vanishing eigenvalue, λ , when the FPE is transformed into a Schrödinger equation [2]. In first approximation, the eigenvalue λ of this bistable potential, is given by,

$$\lambda = \int_0^\infty dx e^{\frac{a}{2c}x^2 + \frac{b}{4c}x^4} \int_x^\infty dy e^{-\frac{a}{2c}y^2 - \frac{b}{4c}y^4}. \quad (46)$$

For the values presented in Fig. 4, λ goes from $\lambda \approx 0.2448$ (for $c = 0.1$) to $\lambda \approx 6 \times 10^{-13}$ (for $c = 10^{-4}$).

V. FINAL REMARKS

In this manuscript we obtained analytical results about the impact of the sampling rate on the KM coefficients directly computed from timeseries.

We analyzed stochastic processes subject to a linear drift, which already comprise a huge variety of processes. We managed to compute exact expressions for the evolution of conditional moments, from which we obtained the finite-time KM coefficients and correlation functions. The first moment and the linear correlation function are both independent of the noise intensity.

We also analyzed standard nonlinear drift cases, where the scenery exhibits a sharp change. The moments are now ruled by a cascade of differential equations which hampers the obtention of exact analytical solutions. Nonetheless, approximate expressions valid for small noise intensity were achieved by means of the adjoint operator approach. Differently from the linear case, the intensity of the noise affects every conditional moment and the correlation function as well. We also showed that by increasing the noise intensity the functional dependence of the KM heads towards the independence regime, which is characterized by a polynomial of the same order. This fact has notorious consequences in time series analysis, since one can be brought onto a situation where independent-like coefficients are obtained, but one is unable to assign this finding to either an improper sample rating or a strong noise intensity.

For sampling rates smaller than the relaxation time, in a steady state approach, our results permit one to sieve the set of processes giving raise to the heuristic stationary probability density function in order to select the appropriate Markovian differential stochastic process and consequently to determine the respective parameter values. Furthermore, it enables the judgement of the validity of the Markovian proposal by supplying precise estimates of higher order KM moments. Otherwise, if the relaxation time is shorter than the sampling rate, the measured KM coefficients will tend to a polynomial of order matching the order of the moment. This functional form is independent of the primary stochastic process, hence introducing uncertainty in the recognition of the process.

Uncertainties might be hedged by inspecting probability densities and correlation functions as well as other measures of dependence such as the relative (Kullback-Leibler) entropy.

Acknowledgements:

CA is grateful to Brazilian agencies Faperj and CNPq for partial financial support and SMDQ acknowledges the

warm hospitality of PUC-Rio and the financial support of the National Institute of Science and Technology for Complex Systems during the early stage of this work.

-
- [1] P. Hanggi and F. Marchesoni (eds), *100 years of Brownian motion*, *Chaos* **15**(2) (2005).
 - [2] H. Risken, *The Fokker-Planck Equation: Methods of Solution and Applications* (Springer-Verlag, Berlin, 1984).
 - [3] C.W. Gardiner, *Handbook of stochastic methods for Physics, Chemistry and Natural Sciences* (Springer-Verlag, Berlin, 1985).
 - [4] A. Einstein, *Ann. der Phys.* **17**, 549 (1905).
 - [5] L. Bachelier, *Annales Scientifiques de l'École Normale Supérieure* **3**, 21 (1900).
 - [6] A.M. van Mourik, A. Daffertshofer and P.J. Beek, *Phys. Lett. A* **351**, 13 (2006).
 - [7] J. Gottschall and J. Peinke, *New Journal of Physics* **10**, 083034 (2008).
 - [8] R. Riera and C. Anteneodo, *J. Stat. Mech.*, P04020 (2010).
 - [9] C. Anteneodo and R. Riera, *Phys. Rev. E* **80**, 031103 (2009).
 - [10] H. Zhou, *J. of Financial Econometrics* **1**, 250 (2003).
 - [11] R. Friedrich, Ch. Renner, M. Siefert and J. Peinke, *Phys. Rev. Lett.* **89**, 149401 (2002).
 - [12] P. Embrechts, C. Klüppelberg and Th. Mikosch, *Modelling Extremal Events: for Insurance and Finance* (Springer-Verlag, Berlin, 1997).
 - [13] S. Siegert, R. Friedrich and J. Peinke, *Phys. Lett. A* **243**, 275 (1998).
 - [14] R. Pythian and W.D. Curtis, *J. Stat. Phys.* **42**, 1019 (1986).
 - [15] R. Friedrich and J. Peinke, *Physica D* **102**, 147 (1997); Ch. Renner, J. Peinke and R. Friedrich, *J. Fluid. Mech.* **433** (2001), 383; C. Anteneodo, E.E. Ferrero, S.A. Canas, *J. Stat. Mech.*, P07026 (2010).

